Int J Appl Earth Obs Geoinformation 82 (2019) 101879

Contents lists available at ScienceDirect

Int J Appl Earth Obs Geoinformation

journal homepage: www.elsevier.com/locate/jag

Using 3D robust smoothing to fill land surface temperature gaps at the continental scale

Hung T. Pham[a,b,*], Seokhyeon Kim[a], Lucy Marshall[a], Fiona Johnson[a]

[a] Water Research Centre, School of Civil and Environmental Engineering, University of New South Wales, Sydney, New South Wales 2052, Australia
[b] The University of Danang, University of Science and Technology, 54 Nguyen Luong Bang, Danang, Viet Nam

ARTICLE INFO

Keywords:
Land surface temperature
MODIS
Gap filling
Reconstruction
Robust smoothing
Australia

ABSTRACT

Land surface temperature (LST) data derived from Moderate Resolution Imaging Spectroradiometer (MODIS) products has been widely applied in environmental studies, and natural disaster management. However missing data in space and time due to cloud contamination, cloud shadows and atmospheric conditions has hindered its application. Accurate gap filling algorithms for a large spatiotemporal scale of LST data are necessary to enhance the utility of this product. This study applied a three-dimensional (3-D) gap-filling method to fill gaps in 9 years of LST data over Australia (2002–2011). As the gap-filling method relies on a smoothing parameter that controls the accuracy of the reconstruction algorithm, we estimated optimal smoothing parameters to separately reconstruct daytime and nighttime LST products. The reconstructed LST were validated against ground-based LST obtained from the OzFlux network and recommendations made on appropriate smoothing parameters. The results demonstrate that the gap-filling algorithm provides an accurate approach to generating reconstructed LST products for a long period over large spatial scales.

1. Introduction

Land surface temperature (LST) is a key variable in the environment because it is closely related to solar radiation, atmospheric conditions and land cover types. Therefore, satellite-derived LST products have been widely used for studies in ecology, hydrology and meteorology (Duan et al., 2018; Spennemann et al., 2018; Zhuang et al., 2016). For example, LST data have been combined with a vegetation index to estimate burn severity and ecosystem recovery (Quintano et al., 2015; Zheng et al., 2016), LST anomalies have been used as markers of earthquakes (Bhardwaj et al., 2017), and differences in LST between daytime and nighttime have been used as an indicator of floods (Parinussa et al., 2016; Pham et al., 2018). LST data have been also used to estimate air temperatures, soil moisture and identify land cover changes (Holzman et al., 2014; Kloog et al., 2014; Wang et al., 2016; Yoo et al., 2018). However the main drawback in the use of currently operational satellite-derived LST data is the large number of gaps in space and time resulting from atmospheric conditions such as clouds and cloud shadows (Li et al., 2018).

There have been many efforts to overcome this issue based on data fusion, empirical relationships to other variables, and temporal or spatial interpolations (Crosson et al., 2012; Duan et al., 2017; Koike, 2013; Weng et al., 2014; Xu and Shen, 2013). However these methods have generally been developed for small regions or short time periods that do not adequately represent the high spatiotemporal variation of LST data (Sun et al., 2017). Recently, spatiotemporal algorithms taking advantages of available data in both time and space to fill gaps in LST data have been designed. Weiss et al. (2014) developed a gap-filling approach for 8-day LST in Africa, but the coarse temporal resolution LST hinders its use in applications such as emergency/risk management which require high frequency data. Daily LST products acquired in 2010 were used by Li et al. (2018) for testing their algorithm, but their study extents are limited over urban and suburban areas in USA. Although these studies have provided a variety of techniques to enhance the applicability of LST products, there remains a need for accurate gap-filling methods for large spatial extents and long time periods without using ancillary datasets.

Garcia (2010) developed a multi-dimensional smoothing algorithm based on the penalised least squares of the discrete cosine transform (DCT-PLS) that explicitly uses available data in both time and space to fill missing satellite data. Garcia (2010) suggested that the benefits of the method are its good computational efficiency and that it is fully automated method that solely relies on a smoothing parameter *s*. If the value of *s* is high, more noise will be removed and thereby the

* Corresponding author at: Water Research Centre, School of Civil and Environmental Engineering, University of New South Wales, Sydney, New South Wales 2052, Australia.
E-mail address: hung.pham@unsw.edu.au (H.T. Pham).

https://doi.org/10.1016/j.jag.2019.05.012
Received 10 January 2019; Received in revised form 10 May 2019; Accepted 10 May 2019

Table 1
Details of validation sites collected from the OzFlux network.

No.	Site ID	Site name	Latitude (°)	Longitude (°)	Elevation	Land cover
1	DR	Daly Regrowth	−14.128	131.383	59 m	Croplands
2	DU	Daly Uncleared	−14.159	131.388	110 m	Woodland savanna
3	SP	Sturt Plains	−17.151	133.350	250 m	Grassland
4	TB	Tumbarumba	−35.657	148.152	1200 m	Forest

reconstructed values are smoother. Garcia (2011) tested the algorithm on a particle image velocimetry (PIV) data with the smooth parameter ranging from 0 to ∞, with the lower bound perfectly reproducing the input data and the upper bound producing a smoothed dataset equal to the arithmetic mean of PIV data. Garcia (2011) suggested that high s can lead to losses of high frequency components and hence the optimal s for the smooth PIV data should be smaller than 0.5 to prevent over-smoothing. Wang et al. (2012) suggested a smoothing parameter value to reconstruct global satellite soil moisture data which enables gap filling while retaining the accuracy of existing information. The smoothing parameter suggested by Wang et al. (2012) for the DCP-PLS method has been widely used to reconstruct soil moisture and vegetation index data (Kim et al., 2018; Lei et al., 2018; Zhang and Weng, 2016).

However to use the DCP-PLS method for other environmental variables, such as LST, which have different physical characteristics to soil moisture or vegetation index data, an optimal smoothing parameter s has to be found. To address this issue, this article aims to find the optimal smoothing parameter for filling gaps in satellite-derived LST products. To do this we adopt the DCP-PLS method with a range of smoothing parameters to fill gaps in 9-year MODIS LST products covering the whole Australia. The aim of the method is to find the optimal smoothing parameter that accurately fills gaps rather than providing a smooth field and so the intention is retain both high and low original LST values rather than reducing the noise in LST data when obtaining the optimal smoothing parameter. Then, the reconstructed LST datasets are validated by comparing to ground-based LST over the study area, which is an advance over previous data validation works for the gap-filling method that has not used any ground data (Wang et al., 2012; Weiss et al., 2014).

2. Data and method

2.1. Study area and data

The study area was selected as the entire continent of Australia (10 °S to 44 °S, 112 °E to 156 °E). The region covers a wide range of climate and land cover types that provides an opportunity to evaluate the gap-filling method for LST products that have high spatiotemporal variation. The dominant climate zones are tropical and summer rainfall in the northern areas, Mediterranean in the southwestern regions, oceanic to humid subtropical in the southeast regions, and arid to semi-arid in the inland area. Land cover types of Australia include forest, shrubland, woodland, grassland, cropland and non-vegetated areas (Peel et al., 2007).

We used daily MODIS LST at 0.05° (MYD11C1, Aqua satellite) (Wan, 2014) for which the approximate local crossing times in the equator are 1:30pm (ascending) and 1:30am (descending) respectively because they are best aligned with the diurnal timing of maximum and minimum air temperature which form part of the method validation. Quality control of these products was applied to select high quality satellite LST data. However, not all cloud contaminated pixels are detected using the cloud mask (Göttsche et al., 2013). To address this, we applied the robust outlier removal method as an additional filter (Duan et al., 2019; Göttsche et al., 2013). The percentages of missing data in the daytime and nighttime LST products over Australia are 28.2% and 32.2% respectively during the 9-year study period (2002–2011). There are spatial and seasonal variations in missing data, for example in northern Australia fewer data are available during the annual wet season. We applied the gap filling method to both daytime and nighttime MODIS LST products for the 9-year period over the study area.

Unlike previous gap-filling studies that have been focused on synthetic gap validation, we used ground-based LSTs as the reference validation data, which were obtained from the Terrestrial Ecosystem Research Network (TERN) OzFlux land-atmosphere observatory network (http://ozflux.org.au). Only ground-based data with good data quality flags were selected. To maximise the available ground-measured data, a 2-year validation period (2009–2010) was used. To ensure that ground-measured data at each flux tower can represent satellite-based data at the pixel scale, we selected only stations with relatively homogeneous land cover. This led to four stations, with a range of land covers, being selected (Table 1). The reference ground LSTs were derived from the upwelling and downwelling longwave radiative fluxes observed by the flux tower data at each station using Eq. (1). This equation has been widely used to validate MODIS LST products (Duan et al., 2019; Wang et al., 2008).

$$LST_{ground} = \left[\frac{L_u - (1-\varepsilon_b)\times L_d}{\varepsilon_b \times \sigma}\right]^{1/4}, \quad (1)$$

where LST_{ground} is ground-based LST (K), L_u is the upwelling longwave radiation (W m^{-2}), L_d is the downwelling longwave radiation (W m^{-2}), σ is the Stefan-Boltzmann constant (5.67×10^{-8} W m^{-2} K^{-4}), and ε_b is the surface broadband emissivity. Here, ε_b was estimated from the Advanced Spaceborne Thermal Emission and Reflection Radiometer (ASTER) Global Emissivity Data (GED) using a linear combination of the five-band emissivity values (bands 10–14) ($\varepsilon_b = 0.197 + 0.025\varepsilon_{10} + 0.057\varepsilon_{11} + 0.237\varepsilon_{12} + 0.333\varepsilon_{13} + 0.146\varepsilon_{14}$) (Cheng et al., 2013).

2.2. LST gap filling method

2.2.1. Three-dimensional robust smoothing

We applied the multi-dimensional robust smooth regression algorithm (Garcia, 2010) to reconstruct LST data (θ). Here, we briefly describe the penalised least square regression based on three-dimensional discrete cosine transforms (DCT-PLS) method. More details of the method are available in Garcia (2010). The DCT-PLST is expressed as

$$F(\hat{\theta}) = \mathrm{RSS} + s\,\mathrm{P}(\hat{\theta}) = \|W^{1/2}\circ(\hat{\theta} - \theta)\|^2 + s\,\|\Delta\hat{\theta}\|^2 \quad (2)$$

where RSS is the residual sum of squares, P is a penalty term and s is a real positive parameter that controls the degree of smoothing. As the value of s increases, the smoothness of $\hat{\theta}$ also increases and vice versa. $||$ $||$ denotes the Euclidean norm, ∘ is element wise product, Δ is the Laplace operator and W is a spatiotemporal binary array ([0, 1]) associated with missing and available data θ_i. The smoothed data $\hat{\theta}$ at k^{th} iteration step can be achieved by rewriting Eq. (2) as

$$\hat{\theta}_{\{k\}} = \mathrm{IDCT}_3\left(\Gamma_3 \circ \mathrm{DCT}_3\left(W\circ(\theta - \hat{\theta}_{\{k-1\}}) + \hat{\theta}_{\{k-1\}}\right)\right) \quad (3)$$

where DCT_3 is three-dimensional discrete cosine transform and $IDCT_3$ is three-dimensional inverse discrete cosine transform. Γ_3 is a three-dimensional tensor ($\Gamma_{i1,\ i2,\ i3}$).

2.2.2. Selection of optimal smoothing parameters and validation

The DCT-LST method depends on the given smooth parameter (s). A higher value of s generates a smoother LST reconstruction and removes the observed high and low LST values. To find an optimal s value for the gap filling purpose rather than the smoothing purpose, we separately tested small s values from 10^{-1} to 10^{-10} with multiplicative increments of 10^{-1} for the daytime and nighttime LST products. Then, the optimal s values were identified by minimising the mean error (ME) between the reconstructed LST and the original LST data for each product. The optimal smoothing parameters were then used to fill missing LST values.

The optimal smoothing parameters were obtained from all observed data which might lead to the overfitting. Although cross validation is generally used to avoid overfitting models for data without gaps, it may result in large errors in data reconstruction with large spatiotemporal gaps (Garcia, 2010). Therefore the ground-measured LSTs were used to evaluate the model performance.

The clear-cloud LSTs and the reconstructed LSTs were validated against ground-based LSTs separately for both daytime and nighttime. Three summary statistics, namely Pearson's correlation coefficient (R), root mean square error (RMSE) and mean bias (Bias) were used to validate these products against ground-based LSTs. The accuracy of the reconstructed LSTs were compared to those of the clear-cloud LSTs to evaluate the model performance.

In addition to the validation of the reconstructed LSTs versus the ground-based LSTs, the daytime/nighttime reconstructed LSTs were compared with the daily maximum/minimum air temperature 0.05° gridded Australian Water Availability Project (AWAP) (Jones et al., 2009) in terms of Pearson's correlation coefficient. The daily AWAP air temperature data are derived by applying a weighted averaging technique to the several thousand climatological station data over the whole of Australia, including topographical corrections and data smoothing processes in data-rich areas.

3. Results and discussion

3.1. Selection of optimal smoothing parameters

The purpose of applying the DCT-PLS method in this study is to fill gaps without losing high and low frequency components of LST rather than smoothing. Thus a small smoothing parameter is required to preserve the information in the original LST data. Wang et al. (2012) suggested an optimal smooth parameter of 10^{-6} for filling gaps in both daytime and nighttime soil moisture products based on a minimum global average reconstruction error. Fig. 1a and b present the relationships between mean errors (ME) of the original and the reconstructed LST data with respect to the ten smoothing parameters tested. As shown, larger smooth parameter values result in higher ME values, and the results demonstrate that the daytime reconstructed LST generally has smaller errors than the nighttime reconstructed LST. These results are consistent with those obtained by Lei et al. (2018). The results indicate that the ME of the daytime and nighttime reconstructed LST product converge to smoothing parameters of 10^{-6} and 10^{-4} respectively. This is likely because the daytime LST data has higher frequency components than the nighttime LST data due to differences in atmospheric conditions (solar radiation, water vapours, temperature and clouds) between daytime and nighttime (Li et al., 2013). Therefore, we suggest applying different smooth parameters for filling gaps in daytime and nighttime products, in which s is smaller than or equal to 10^{-6} for daytime products and $s \leq 10^{-4}$ for nighttime products (Fig. 1a and b). These optimal s values were defined for the whole country for all land covers. Although different continents have different climate conditions and land covers, the findings over Australia provide a valuable reference for future studies that might apply a similar approach to fill gaps of LST in other parts of the world.

As depicted in Fig. 1c and d, there may be large gaps in the original daytime and nighttime LST, which result from cloud masks and the satellite swath patterns. Fig. 1e and f show how the gaps on the date of interest were accurately filled by the DCT-PLS method using the optimal smooth parameters. The reconstructed LST has some discontinuous surfaces between the original and reconstructed LST data, especially over the large gaps (i.e. over the satellite swath gap in the red ovals presented in Fig. 1d and f). This is because the DCT-PLS algorithm tends to use low frequency climatology to fill large gaps (Wang et al., 2012). Therefore, with large spatiotemporal gaps in LST over other continents shown in Figure S1 in the Supplementary Material, caution should be applied when using the DCT-PLS algorithm in such regions. Similar to previous research, further work is required to assess the effects of these large spatiotemporal gaps on the accuracy of the LST reconstruction. For such large spatiotemporally continuous gaps, the predicted LSTs should be compared to available ground-based LSTs or air temperature to assess the accuracy of the prediction model over such regions. In the following section, the reconstructed LST data using the selected optimal smooth parameters for daytime and nighttime LST data are compared to the ground-measured LSTs and the AWAP air temperature to validate the performance of the DCT-PLS method over the continental scale with different climate zones and land covers.

3.2. Validation

The validation results using the ground-based LSTs are presented in Fig. 2. When compared to ground-based LSTs (cross marks in Fig. 2), the accuracy of the MODIS LST can be assessed for both daytime and nighttime data. The biases of the clear-cloud LSTs during the nighttime were smaller than 2 K and lower than those in daytime for three of the four sites, the exception being the DU site (Fig. 2c and d), similar to the findings of Li et al. (2014) and Bosilovich (2006). The mixture of woodlands and parts of grasslands at satellite pixel scale over the DU site could lead to high variations of the clear-cloud LSTs in nighttime at this site (Fig. 2d). The higher RMSE values (> 2 K) of the clear-cloud daytime LST at the DR site (cropland) and the SP site (woodland) suggest that there may be heterogeneous land use at these sites, with possible variations of farming activities over the DR site or seasonal changes in vegetation canopy over the SP site.

The most important results in Fig. 2 are the performance of the reconstructed LST data (filled circles in Fig. 2). In general the gap-filled data has similar performance to the clear-cloud LST, with generally slightly higher errors (RMSE between 2 K and 3.9 K). The exception is that for the TB site where the RMSE of the reconstructed LST data is substantially higher than the clear-sky data (Fig. 2g). It should be noted that the DCT-PLS model uses all data with higher weights assigned to closer points in space and time. Therefore, the errors of the reconstructed LST at each site could be caused not only by the model uncertainty but also the errors of the clear-cloud LSTs around the site. Although land cover at the satellite pixel scale over the TB site is homogeneous (forest), land covers at neighbouring pixels surrounding the TB site are a mixture of bare soils, agricultural land and pervious area which frequently have higher daytime LST compared to high density vegetation areas. This could explain why the clear-cloud LST had high accuracy, whereas the reconstructed LST was overestimated at the TB site. These findings suggest that the weight of the DCT-PLS model should be defined considering land covers together with the distances and this could be a potential for future study. As with the clear-cloud LSTs, the predicted nighttime LSTs performed better than the gap-filled daytime LSTs. An explanation of this is that LST of these land covers are usually less variations in nighttime. In summary, this indicates that the gap-filling method provides reasonable results when compared to the performance of the clear-cloud LST at the four validation sites.

As a more comprehensive continent-wide comparison than the four ground-based LST sites assessed above, the reconstructed LST data has been correlated against AWAP maximum/minimum air temperature

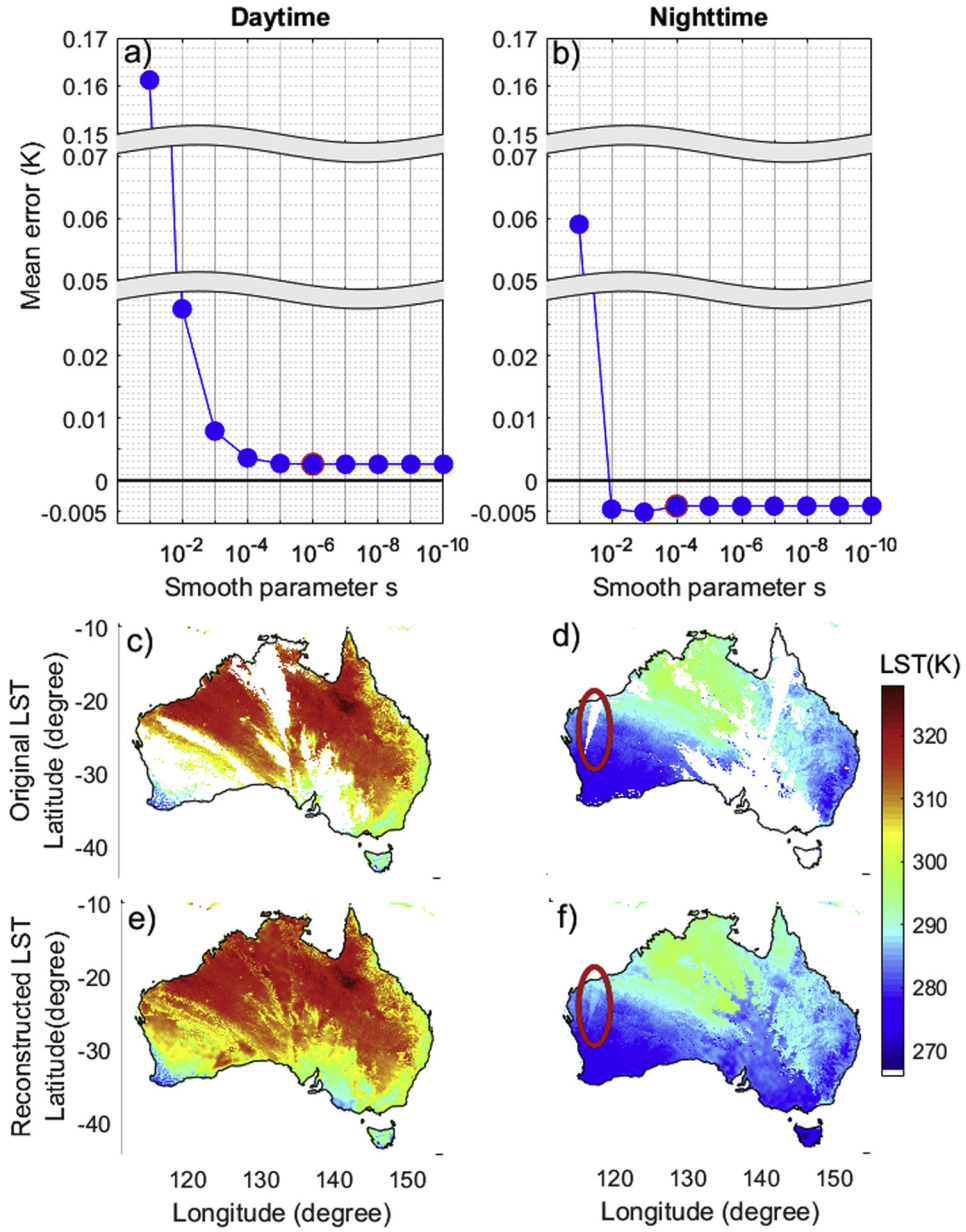

Fig. 1. Mean error between the original LST and the reconstructed LST using the optimal smooth parameter for a) daytime and b) nighttime LST data. Original LST data with gaps in c) daytime and d) nighttime in 15/09/2002. Reconstructed LST data in e) daytime and f) nighttime using the DCT-PLS with the optimal *s* values.

(Fig. 3a and b). The correlation is higher than 0.8 for 74% and 77% of the daytime and nighttime pixels respectively. High correlations were found in south-eastern and –western Australia for the daytime LST data (Fig. 3a) and in north-eastern and –western Australia for the nighttime product (Fig. 3b). Almost all large filled-gaps in the centre of the country have good agreement with the ground air temperature. The results suggest good predictive skill of the DCT-PLST gap-filling algorithm for large spatiotemporal LST datasets over different climate zones and land covers.

For the daytime product (Fig. 3a) in northern Australia, the effects of daytime clouds and the summer monsoon leads to fewer available data and the correlation is lower in this region. For the nighttime product (Fig. 3b), lower correlations were found in the south of the country. Lower correlations along coastal regions may be because air temperature is not as strongly related to ground temperature due to wind and humidity effects in this region. In addition, because the DCT-PLS method uses the entire data with weights of zero assigned to missing values to fill gaps, the reconstructed LST along the boundaries (i.e. coastal lines) have low correlations due to the smaller number of available data points over land. This limitation may be reduced by using a longer observation period or by merging this data with MODIS/Terra LST products before implementing the gap filling. Further research is required to investigate these hypotheses.

4. Conclusions

Given the important role of LST data in environmental processes, filling gaps in these datasets is vital to ensure that studies using this data can be as effective as possible. The aim of this study was to identify an appropriate smoothing parameter for the DCT-PLS algorithm to fill gaps in space and time in LST datasets derived from satellites. This study has identified the optimal smooth parameters as 10^{-6} and 10^{-4} for the daytime and nighttime products respectively, which control the degree of smoothness in the algorithm. These optimal parameters retain the high frequency components of the original LST data and provide realistically reconstructed LST data in the large gaps. The validation

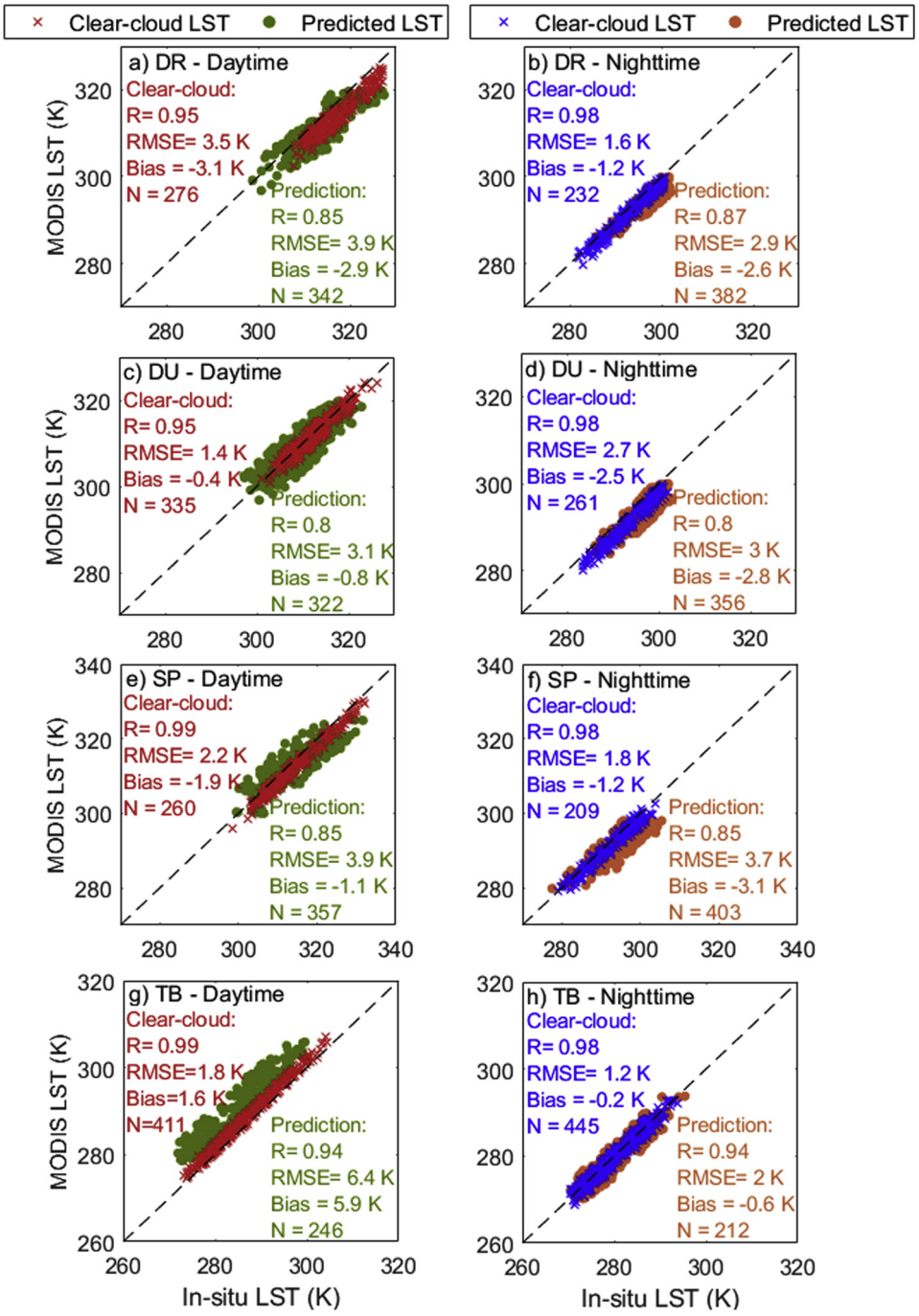

Fig. 2. Scatter plots of clear-cloud MODIS LST and predicted LST versus ground-based LST during daytime (left panels) and nighttime (right panels) at (a and b) DR, (c and d) DU, (e and f) SP, and (g and h) TB.

results indicated that the reconstructed products have strong correlations with ground-measured LSTs at four validation sites as well as continent-wide maximum/minimum air temperatures. One of the advantages of the method is that it does not rely on alternative geospatial datasets to fill gaps thereby avoiding additional uncertainty that would be introduced by ancillary datasets.

Acknowledgements

This study was funded by the Australian Research Council as part of the Discovery Project DP140102394. Hung Pham is funded by The University of New South Wales Tuition Fee Scholarship (TFS). Seokhyeon Kim is supported by a Linkage Project LP160100620 funded by the Australian Research Council, Sydney Water and WaterNSW. A/Prof Marshall is additionally supported through an Australian Research Council Future FellowshipFT120100269. We wish to thank Damien Garcia who developed the smoothing algorithm (http://www.biomecardio.com/matlab/smoothn.html), NASA and OzFlux project for providing free satellite data and ground skin temperature datasets used in this research.

Appendix A. Supplementary data

Supplementary material related to this article can be found, in the online version, at doi:https://doi.org/10.1016/j.jag.2019.05.012.

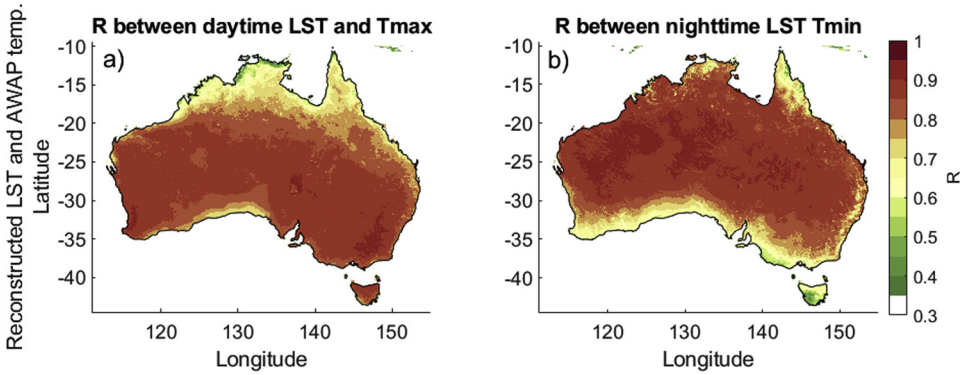

Fig. 3. Correlation between the reconstructed LST and the AWAP a) daytime LST and maximum air temperature, b) nighttime LST and minimum air temperature.

References

Bhardwaj, A., Singh, S., Sam, L., Joshi, P., Bhardwaj, A., Martín-Torres, F.J., Kumar, R., 2017. A review on remotely sensed land surface temperature anomaly as an earthquake precursor. Int. J. Appl. Earth Obs. Geoinf. 63, 158–166.

Bosilovich, M.G., 2006. A comparison of MODIS land surface temperature with in situ observations. Geophys. Res. Lett. 33.

Cheng, J., Liang, S., Yao, Y., Zhang, X., 2013. Estimating the optimal broadband emissivity spectral range for calculating surface longwave net radiation. IEEE Geosci. Remote. Sens. Lett. 10, 401–405.

Crosson, W.L., Al-Hamdan, M.Z., Hemmings, S.N., Wade, G.M., 2012. A daily merged MODIS Aqua–Terra land surface temperature data set for the conterminous United States. Remote Sens. Environ. 119, 315–324.

Duan, S.-B., Li, Z.-L., Leng, P., 2017. A framework for the retrieval of all-weather land surface temperature at a high spatial resolution from polar-orbiting thermal infrared and passive microwave data. Remote Sens. Environ. 195, 107–117.

Duan, S.-B., Li, Z.-L., Li, H., Göttsche, F.-M., Wu, H., Zhao, W., Leng, P., Zhang, X., Coll, C., 2019. Validation of Collection 6 MODIS land surface temperature product using in situ measurements. Remote Sens. Environ. 225, 16–29.

Duan, S.-B., Li, Z.-L., Wu, H., Leng, P., Gao, M., Wang, C., 2018. Radiance-based validation of land surface temperature products derived from Collection 6 MODIS thermal infrared data. Int. J. Appl. Earth Obs. Geoinf. 70, 84–92.

Garcia, D., 2010. Robust smoothing of gridded data in one and higher dimensions with missing values. Comput. Stat. Data Anal. 54, 1167–1178.

Garcia, D., 2011. A fast all-in-one method for automated post-processing of PIV data. Exp. Fluids 50, 1247–1259.

Göttsche, F.-M., Olesen, F.-S., Bork-Unkelbach, A., 2013. Validation of land surface temperature derived from MSG/SEVIRI with in situ measurements at Gobabeb, Namibia. Int. J. Remote Sens. 34, 3069–3083.

Holzman, M.E., Rivas, R., Piccolo, M.C., 2014. Estimating soil moisture and the relationship with crop yield using surface temperature and vegetation index. Int. J. Appl. Earth Obs. Geoinf. 28, 181–192.

Jones, D.A., Wang, W., Fawcett, R., 2009. High-quality spatial climate data-sets for Australia. Aust. Meteorol. Oceanogr. J. 58, 233.

Kim, S., Paik, K., Johnson, F.M., Sharma, A., 2018. Building a flood-warning framework for ungauged locations using low resolution, open-access remotely sensed surface soil moisture, precipitation, soil, and topographic information. IEEE J. Sel. Topics Appl. Earth Observ. Remote Sens. 11, 375–387.

Kloog, I., Nordio, F., Coull, B.A., Schwartz, J., 2014. Predicting spatiotemporal mean air temperature using MODIS satellite surface temperature measurements across the Northeastern USA. Remote Sens. Environ. 150, 132–139.

Koike, T., 2013. Soil Moisture Algorithm, Descriptions of GCOM-W1 AMSR2 (Rev. A). Earth Observation Research Center, Japan Aerospace Exploration Agency pp. 8-1˜8-13.

Lei, F., Crow, W.T., Shen, H., Su, C.-H., Holmes, T.R.H., Parinussa, R.M., Wang, G., 2018. Assessment of the impact of spatial heterogeneity on microwave satellite soil moisture periodic error. Remote Sens. Environ. 205, 85–99.

Li, H., Sun, D., Yu, Y., Wang, H., Liu, Y., Liu, Q., Du, Y., Wang, H., Cao, B., 2014. Evaluation of the VIIRS and MODIS LST products in an arid area of Northwest China. Remote Sens. Environ. 142, 111–121.

Li, X., Zhou, Y., Asrar, G.R., Zhu, Z., 2018. Creating a seamless 1km resolution daily land surface temperature dataset for urban and surrounding areas in the conterminous United States. Remote Sens. Environ. 206, 84–97.

Li, Z.-L., Tang, B.-H., Wu, H., Ren, H., Yan, G., Wan, Z., Trigo, I.F., Sobrino, J.A., 2013. Satellite-derived land surface temperature: current status and perspectives. Remote Sens. Environ. 131, 14–37.

Parinussa, R.M., Lakshmi, V., Johnson, F.M., Sharma, A., 2016. A new framework for monitoring flood inundation using readily available satellite data. Geophys. Res. Lett. 43, 2599–2605.

Peel, M.C., Finlayson, B.L., McMahon, T.A., 2007. Updated world map of the Köppen-Geiger climate classification. Hydrol. Earth Syst. Sci. 11, 1633–1644.

Pham, H.T., Marshall, L., Johnson, F., Sharma, A., 2018. Deriving daily water levels from satellite altimetry and land surface temperature for sparsely gauged catchments: a case study for the Mekong River. Remote Sens. Environ. 212, 31–46.

Quintano, C., Fernández-Manso, A., Calvo, L., Marcos, E., Valbuena, L., 2015. Land surface temperature as potential indicator of burn severity in forest Mediterranean ecosystems. Int. J. Appl. Earth Obs. Geoinf. 36, 1–12.

Spennemann, P., Salvia, M., Ruscica, R., Sörensson, A., Grings, F., Karszenbaum, H., 2018. Land-atmosphere interaction patterns in southeastern South America using satellite products and climate models. Int. J. Appl. Earth Obs. Geoinf. 64, 96–103.

Sun, L., Chen, Z., Gao, F., Anderson, M., Song, L., Wang, L., Hu, B., Yang, Y., 2017. Reconstructing daily clear-sky land surface temperature for cloudy regions from MODIS data. Comput. Geosci. 105, 10–20.

Wan, Z., 2014. New refinements and validation of the collection-6 MODIS land-surface temperature/emissivity product. Remote Sens. Environ. 140, 36–45.

Wang, G., Garcia, D., Liu, Y., De Jeu, R., Dolman, A.J., 2012. A three-dimensional gap filling method for large geophysical datasets: application to global satellite soil moisture observations. Environ. Model. Softw. 30, 139–142.

Wang, J., Qingming, Z., Guo, H., Jin, Z., 2016. Characterizing the spatial dynamics of land surface temperature–impervious surface fraction relationship. Int. J. Appl. Earth Obs. Geoinf. 45, 55–65.

Wang, W., Liang, S., Meyers, T., 2008. Validating MODIS land surface temperature products using long-term nighttime ground measurements. Remote Sens. Environ. 112, 623–635.

Weiss, D.J., Atkinson, P.M., Bhatt, S., Mappin, B., Hay, S.I., Gething, P.W., 2014. An effective approach for gap-filling continental scale remotely sensed time-series. ISPRS J. Photogramm. Remote. Sens. 98, 106–118.

Weng, Q., Fu, P., Gao, F., 2014. Generating daily land surface temperature at Landsat resolution by fusing Landsat and MODIS data. Remote Sens. Environ. 145, 55–67.

Xu, Y., Shen, Y., 2013. Reconstruction of the land surface temperature time series using harmonic analysis. Comput. Geosci. 61, 126–132.

Yoo, C., Im, J., Park, S., Quackenbush, L.J., 2018. Estimation of daily maximum and minimum air temperatures in urban landscapes using MODIS time series satellite data. ISPRS J. Photogramm. Remote. Sens. 137, 149–162.

Zhang, L., Weng, Q., 2016. Annual dynamics of impervious surface in the Pearl River Delta, china, from 1988 to 2013, using time series Landsat imagery. ISPRS J. Photogramm. Remote. Sens. 113, 86–96.

Zheng, Z., Zeng, Y., Li, S., Huang, W., 2016. A new burn severity index based on land surface temperature and enhanced vegetation index. Int. J. Appl. Earth Obs. Geoinf. 45, 84–94.

Zhuang, Q., Wu, B., Yan, N., Zhu, W., Xing, Q., 2016. A method for sensible heat flux model parameterization based on radiometric surface temperature and environmental factors without involving the parameter KB− 1. Int. J. Appl. Earth Obs. Geoinf. 47, 50–59.